

Study of chiral symmetry restoration in linear and nonlinear $O(N)$ models using the auxiliary field method

Elina Seel^a, Stefan Strüber^a, Francesco Giacosa^a, and Dirk H. Rischke^{a,b}

^a*Institute for Theoretical Physics, Goethe University,
Max-von-Laue-Str. 1, D-60438 Frankfurt am Main, Germany and*
^b*Frankfurt Institute for Advanced Studies, Goethe University,
Ruth-Moufang-Str. 1, D-60438 Frankfurt am Main, Germany*

We consider a linear $O(N)$ model and introduce an auxiliary field to eliminate the scalar self-interaction. Using a suitable limiting process this model can be continuously transformed into the nonlinear $O(N)$ model. We study this model at nonzero temperature applying the CJT formalism. Due to the presence of the auxiliary field the effective potential and, consequently, the equations for the order parameter and the masses of the particles turn out to be different from those previously obtained in similar studies of the linear and nonlinear $O(N)$ models. The order of the chiral phase transition depends sensitively on the choice of the renormalization scheme. In the linear version of the model and for explicitly broken chiral symmetry, it turns from crossover to first order as the mass of the σ particle increases. In the nonlinear case, the order of the phase transition turns out to be of first order. In the region where the parameter space of the model allows for physical solutions of the gap equations, Goldstone's theorem is always fulfilled.

I. INTRODUCTION

Scalar models in $d + 1$ space-time dimensions with orthogonal symmetry are widely used in many areas of physics. Some applications of these $O(N)$ models are quantum dots, high-temperature superconductivity, low-dimensional systems, polymers, organic metals, biological molecular arrays, and chains. In this paper, we focus on a physical system consisting of interacting pions and sigma mesons at nonzero temperature T . For three spatial dimensions, $d = 3$, an analytical solution to this model does not exist. Thus, one has to use many-body approximation schemes in order to compute quantities of interest, such as the effective potential, the order parameter, and the masses of the particles as a function of T . As an approximation scheme never gives the exact solution, it is of interest to compare different schemes and assess their physical relevance.

For $N = 4$ the $O(N)$ symmetry group for the internal degrees of freedom is locally isomorphic to the chiral $SU(2)_R \times SU(2)_L$ symmetry group of quantum chromodynamics (QCD) with $N_f = 2$ massless quark flavors. The phenomena of low-energy QCD are largely governed by chiral symmetry.

In the case of zero quark masses the QCD Lagrangian is invariant under $U(N_f)_R \times U(N_f)_L$ transformations, N_f being the number of quark flavors. However, the true symmetry of QCD is only $U(N_f)_V \times SU(N_f)_A$, because of the axial anomaly which explicitly breaks $U(1)_A$ due nontrivial topological effects [1]. For N_f nonzero but degenerate quark masses, the $SU(N_f)_A$ symmetry is explicitly broken, such that QCD has only a $U(N_f)_V$ flavor symmetry. In reality, different quark flavors have different masses, reducing the symmetry of QCD to $U(1)_V$, which corresponds to baryon number conservation. In the vacuum, the axial $SU(N_f)_A$ symmetry is also spontaneously broken by a non-vanishing expectation value of the quark condensate $\langle \bar{q}q \rangle \neq 0$ [2]. According to Goldstone's theorem, this leads to $N_f^2 - 1$ Goldstone bosons.

The chiral symmetry is restored at a temperature T which for dimensional reasons is expected to be of the order of $\Lambda_{QCD} \sim 200$ MeV. This scenario is indeed confirmed by lattice simulations, in which a crossover phase transition at $T_c \sim 150$ MeV has been observed [3].

For vanishing quark masses, the high- and the low-temperature phases of QCD have different symmetries, and therefore must be separated by a phase transition. The order of this chiral phase transition is determined by the global symmetry of the QCD Lagrangian; for $U(N_f)_V \times U(N_f)_A$, the transition is of first order if $N_f \geq 2$; for $U(N_f)_V \times SU(N_f)_A$ the transition can be of second order if $N_f \leq 2$ [4]. If the quark masses are nonzero, the second-order phase transition becomes crossover.

The calculation of hadronic properties at nonzero temperature faces serious technical difficulties. For a nonconvex effective potential standard perturbation theory cannot be applied. Furthermore, at nonzero temperature an additional scale is introduced which invalidates the usual power counting in terms of the coupling constant [5]. A consistent calculation to a given order in the coupling constant then may require a resummation of whole classes of diagrams [6].

A convenient technique to perform such a resummation and thus arrive at a particular many-body approximation scheme is the so-called two-particle irreducible (2PI) or Cornwall-Jackiw-Tomboulis (CJT) formalism [7, 8], which is a relativistic generalization of the Φ -functional formalism [9, 10]. The CJT formalism extends the concept of

the generating functional $\Gamma[\phi]$ for one-particle irreducible (1PI) Green's functions to that for 2PI Green's functions $\Gamma[\phi, G]$, where ϕ and G are the one- and two-point functions. The central quantity in this formalism is the sum of all 2PI vacuum diagrams, $\Gamma_2[\phi, G]$. Any many-body approximation scheme can be derived as a particular truncation of $\Gamma_2[\phi, G]$.

An advantage of the CJT formalism is that it avoids double counting and fulfills detailed balance relations and thus is thermodynamically consistent. Another advantage is that the Noether currents are conserved for an arbitrary truncation of Γ_2 , as long as the one- and two-point functions transform as rank-1 and rank-2 tensors. A disadvantage is that Ward-Takahashi identities for higher-order vertex functions are no longer fulfilled [11]. As a consequence, Goldstone's theorem is violated [12, 13]. A strategy to restore Goldstone's theorem is to perform a so-called “external” resummation of random-phase approximation diagrams with internal lines given by the full propagators of the approximation used in the CJT formalism [11].

In the literature different many-body approximations have been applied to examine the thermodynamical behavior of the $O(N)$ model in its linear and nonlinear version. In Ref. [14] optimized perturbation theory was used to compute the effective potential, spectral functions, and dilepton emission rates. The CJT formalism has been applied to study the thermodynamics of the $O(N)$ model in the so-called “double-bubble” approximation [12, 13, 15–23], in Ref. [24] sunset-type diagrams have been included. The $1/N$ expansion has also been used several times to study various properties of the $O(N)$ model at zero [25, 26] and nonzero [27–30] temperature.

Here we calculate the effective potential, the masses, the condensate, and the pressure of the $O(N)$ model at nonzero T both in the linear and nonlinear cases by making use of an auxiliary field. This field allows us to obtain the nonlinear version of the model by a well-defined limiting process from the linear version. We find that to lowest loop order, $\Gamma_2 = 0$. Nevertheless, when using the gap equation for the auxiliary field, the gap equations for pions and sigma mesons still contain self-consistently computed loops. Although qualitatively similar to the standard double-bubble approximation in the treatment without auxiliary field, the gap equations are quantitatively different and thus lead to different results for the order parameter and the masses of the particles as a function of T .

The order of the chiral phase transition depends sensitively on the choice of renormalization scheme. In the linear version of the model and for explicitly broken chiral symmetry, it turns from crossover to first order as the mass of the σ particle increases. In the counter-term renormalization scheme, this transition happens for smaller values of the σ meson than in the so-called trivial renormalization scheme. In the nonlinear case the phase transition is of first order. Besides, in the region where the parameter space of the model allows for physical solutions of the gap equations, Goldstone's theorem is always respected.

The manuscript is organized as follows: in Sec. II the linear and nonlinear versions of the model are presented and how they can be related with the help of an auxiliary field. In Sec. III the effective potential and the gap equations are derived. In Sec. IV the results are presented for the linear and nonlinear versions of the model in the case of non-vanishing and vanishing explicit symmetry breaking. Section V concludes this paper with a summary of our results and an outlook for further studies.

We use the imaginary-time formalism to compute quantities at nonzero temperature. Our notation is

$$\int_k f(k) = T \sum_{n=-\infty}^{n=\infty} \int \frac{d^3 k}{(2\pi)^3} f(2\pi i n T, \vec{k}). \quad (1)$$

We use units $\hbar = c = k_B = 1$. The metric tensor is $g^{\mu\nu} = \text{diag}(1, -1, -1, -1)$.

II. THE $O(N)$ MODEL

The generating functional of the σ -model with $O(N)$ symmetry at nonzero temperature T is given by

$$Z_L(\varepsilon, h) = N \int \mathcal{D}\alpha \mathcal{D}\Phi \exp \left(\int_0^{1/T} d\tau \int_V d^3 x \mathcal{L}_{\sigma-\alpha} \right), \quad (2)$$

with the Lagrangian

$$\mathcal{L}_{\sigma-\alpha} = \frac{1}{2} (\partial_\mu \Phi)^2 - U(\Phi, \alpha), \quad U(\Phi, \alpha) = \frac{i}{2} \alpha (\Phi^2 - v_0^2) + \frac{N\varepsilon}{8} \alpha^2 - h\sigma, \quad (3)$$

where $\Phi^2 = \Phi^t \Phi$, $\Phi^t = (\sigma, \pi_1, \dots, \pi_{N-1})$ and α is an auxiliary field serving as a Lagrange multiplier. One can obtain the generating functional of the $O(N)$ model in its familiar form by integrating out the field α :

$$Z_L(\varepsilon, h) = \int \mathcal{D}\Phi \exp \left(\int_0^{1/T} d\tau \int_V d^3 x \mathcal{L}_\sigma \right), \quad (4)$$

with the Lagrangian

$$\mathcal{L}_\sigma = \frac{1}{2} (\partial_\mu \Phi)^2 - \frac{1}{2N\varepsilon} (\Phi^2 - v_0^2)^2 + h\sigma . \quad (5)$$

As one can see, the potential of the model exhibits the typical tilted Mexican hat shape, with the parameter $1/\varepsilon$ being the coupling constant, h the parameter for explicit symmetry breaking, and v_0 the vacuum expectation value (v.e.v.) of Φ . The π_i fields can be identified as the pseudo-Goldstone fluctuations.

Another way to see the equivalence to the standard form of the $O(N)$ model is to use the equation of motion for the auxiliary field α ,

$$\frac{\delta \mathcal{L}_{\sigma-\alpha}}{\delta \alpha} - \partial_\mu \frac{\delta \mathcal{L}_{\sigma-\alpha}}{\delta \partial_\mu \alpha} = 0 \quad \Longrightarrow \quad i\alpha = \frac{2}{N\varepsilon} (\Phi^2 - v_0^2) . \quad (6)$$

When plugging the latter into $\mathcal{L}_{\sigma-\alpha}$ one recovers, as expected, the familiar Lagrangian \mathcal{L}_σ .

The advantage of the representation (2) of the generating functional of the *linear* σ -model is that, by taking the limit $\varepsilon \rightarrow 0^+$, one naturally obtains the *nonlinear* version of the σ -model with the fields constrained by the condition $\Phi^2 = v_0^2$. In fact

$$\begin{aligned} Z_{NL}(h) &= \lim_{\varepsilon \rightarrow 0^+} Z_L(\varepsilon, h) = \lim_{\varepsilon \rightarrow 0^+} N \int \mathcal{D}\alpha \mathcal{D}\Phi \exp \left[\int_0^{1/T} d\tau \int_V d^3x \mathcal{L}_{\sigma-\alpha} \right] \\ &= \int \mathcal{D}\Phi \delta(\Phi^2 - v_0^2) \exp \left[\int_0^{1/T} d\tau \int_V d^3x \left(\frac{1}{2} (\partial_\mu \Phi)^2 + h\sigma \right) \right] , \end{aligned} \quad (7)$$

because $\delta(\Phi^2 - v_0^2)$ can be identified with

$$\delta(\Phi^2 - v_0^2) = \lim_{\varepsilon \rightarrow 0^+} N \int \mathcal{D}\alpha \exp \left\{ - \int_0^{1/T} d\tau \int_V d^3x \left[\frac{i}{2} \alpha (\Phi^2 - v_0^2) + \frac{N\varepsilon}{8} \alpha^2 \right] \right\} , \quad (8)$$

which is the mathematically well-defined (i.e., convergent) form of the usual representation of the functional δ -function. Equation (8) ensures that the Mexican hat potential becomes infinitely steep and, consequently, the mass of the radial degree of freedom infinite.

Note that in some previous studies of the $O(N)$ nonlinear σ -model [27, 28], the ε -dependence in Eq. (8) was not appropriately handled: there, the limit $\varepsilon \rightarrow 0^+$ was exchanged with the functional $\mathcal{D}\alpha$ integration, effectively setting $\varepsilon = 0$ in the exponent. This, however, is incorrect, since the additional term $\sim \varepsilon \alpha^2$ is essential to establish the link between the linear model and the nonlinear one. Without this term, an integration over the auxiliary field does not give the correct potential of the linear model. Thus, for a proper construction of the nonlinear limit of the $O(N)$ model the ε -dependence must be included.

III. THE EFFECTIVE POTENTIAL AND GAP EQUATIONS

In this work we study the thermodynamical behavior of the $O(N)$ σ -model, and in particular the temperature dependence of the masses of the modes and of the condensate. To this end one has to apply methods that go beyond the standard loop expansion which is not applicable when the effective potential is not convex [31], as is the case here because of spontaneous chiral symmetry breaking. A method that allows to compute quantities like the effective potential, the masses, and the order parameter at nonzero temperature is provided by the Cornwall-Jackiw-Tomboulis (CJT) formalism [7]. Within this formalism, the effective potential V is given by

$$V_{\text{eff}} = U(\phi) + \frac{1}{2} \int_k [\ln G^{-1}(k) + D^{-1}(k; \phi) G(k) - 1] + V_2(\phi, G) , \quad (9)$$

where the one-point function ϕ and the connected two-point function $G(k)$ are determined by the extrema of the effective potential,

$$\frac{\delta V_{\text{eff}}}{\delta \phi} = 0 , \quad \frac{\delta V_{\text{eff}}}{\delta G(k)} = 0 . \quad (10)$$

In Eq. (9), $U(\phi)$ is the tree-level potential, $D^{-1}(k; \phi)$ is the tree-level propagator in momentum space, and $V_2(\phi, G)$ contains all two-particle irreducible diagrams.

In our case, the fields occurring in the Lagrangian are $\sigma, \boldsymbol{\pi} \equiv (\pi_1, \dots, \pi_{N-1})^t$, as well as the auxiliary field α . The tree-level potential is given by

$$U = \frac{i}{2}(\alpha_0 + \alpha)(\sigma^2 + \boldsymbol{\pi}^2 + 2\sigma\phi + \phi^2 - v_0^2) + \frac{N\varepsilon}{8}(\alpha_0 + \alpha)^2 - h(\phi + \sigma), \quad (11)$$

where we have already anticipated that the fields σ and α attain non-vanishing vacuum expectation values, $\sigma \rightarrow \phi + \sigma$ and $\alpha \rightarrow \alpha_0 + \alpha$, respectively. The shift produces a bilinear mixing term, $i\alpha\sigma\phi$, which renders the mass matrix non-diagonal in the fields σ and α . There are various ways to treat this mixing term, for instance keeping this term and allowing for a non-diagonal propagator which mutually transforms the fields σ and α into each other. There is, however, a simple method to eliminate this unphysical mixing: we perform a further shift,

$$\alpha \longrightarrow \alpha - 4\frac{i\phi}{N\varepsilon}\sigma. \quad (12)$$

Using the fact that linear terms in the fields vanish on account of the definition of the vacuum expectation values, $dU/d\phi \equiv 0$, $dU/d\alpha_0 \equiv 0$, the resulting expression of the Lagrangian reads

$$\begin{aligned} \mathcal{L}_{\sigma-\alpha} = & \frac{1}{2}(\partial_\mu\sigma)^2 + \frac{1}{2}(\partial_\mu\boldsymbol{\pi})^2 - \frac{1}{2}\left(i\alpha_0 + \frac{4\phi^2}{N\varepsilon}\right)\sigma^2 - \frac{1}{2}(i\alpha_0)\boldsymbol{\pi}^2 - \frac{1}{2}\frac{N\varepsilon}{4}\alpha^2 \\ & - \frac{i}{2}\alpha(\sigma^2 + \boldsymbol{\pi}^2) - \frac{2\phi}{N\varepsilon}\sigma(\sigma^2 + \boldsymbol{\pi}^2) - \frac{i}{2}\alpha_0(\phi^2 - v_0^2) - \frac{N\varepsilon}{8}\alpha_0^2 + h\phi. \end{aligned} \quad (13)$$

One can immediately deduce the inverse tree-level propagators and the tree-level masses:

$$D_i^{-1}(k; \phi, \alpha_0) = -k^2 + m_i^2; \quad i = \sigma, \boldsymbol{\pi}, \quad (14)$$

$$m_\sigma^2 = i\alpha_0 + \frac{4\phi^2}{N\varepsilon}, \quad m_\pi^2 = i\alpha_0, \quad (15)$$

$$D_\alpha^{-1}(k; \phi, \alpha_0) = m_\alpha^2 = \frac{N\varepsilon}{4}. \quad (16)$$

The shift (12) has two features: the Jacobian associated with the transformation is unity, thus the functional integration in Eq. (7) remains unaffected. Furthermore, this shift generates a term in the σ -mass, which diverges in the limit $\varepsilon \rightarrow 0^+$, see Eq. (15). This is expected, since the σ -particle becomes infinitely heavy in the nonlinear version of the $O(N)$ model.

We now turn to the effective potential,

$$\begin{aligned} V_{\text{eff}}(\phi, \alpha_0, G_\sigma, G_\pi, G_\alpha) = & \frac{i}{2}\alpha_0(\phi^2 - v_0^2) + \frac{N\varepsilon}{8}\alpha_0^2 - h\phi \\ & + \frac{1}{2} \sum_{i=\sigma, \pi, \alpha} \int_k [\ln G_i^{-1}(k) + D_i^{-1}(k; \phi, \alpha_0) G_i(k) - 1] + V_2. \end{aligned} \quad (17)$$

We now make an important observation. The Lagrangian (13) only contains three-point interaction terms between the fields $\sigma, \boldsymbol{\pi}, \alpha$. Therefore, the lowest-order contribution to V_2 is a two-loop “sunset”-type diagram constructed from two three-point vertices. There is no two-loop diagram of double-bubble-type which would require the existence of a four-point vertex. If we restrict ourselves to a many-body approximation where the self-energy of the particles is independent of momentum, we have to neglect sunset-type diagrams (as well diagrams of higher loop order), and the contribution of V_2 to the CJT effective potential vanishes trivially. As a consequence, the effective potential only contains tree-level and one-loop terms.

Using the stationary conditions for the effective potential

$$\frac{\delta V_{\text{eff}}}{\delta \phi} = 0, \quad \frac{\delta V_{\text{eff}}}{\delta \alpha_0} = 0, \quad \frac{\delta V_{\text{eff}}}{\delta G_i(k)} = 0; \quad i = \sigma, \boldsymbol{\pi}, \alpha, \quad (18)$$

one derives the following equations for the condensates,

$$h = i\alpha_0\phi + \frac{4\phi}{N\varepsilon} \int_k G_\sigma(k), \quad (19)$$

$$i\alpha_0 = \frac{2}{N\varepsilon} \left[\phi^2 - v_0^2 + \int_k G_\sigma(k) + (N-1) \int_k G_\pi(k) \right], \quad (20)$$

and full propagators,

$$G_i^{-1}(k) = -k^2 + M_i^2 = D_i^{-1}(k; \phi, \alpha_0), \quad M_i^2 \equiv m_i^2; \quad i = \sigma, \pi, \alpha. \quad (21)$$

Since V_2 vanishes in our approximation, the contribution from the 1PI self-energy, $\Pi_i \equiv -2\partial V_2/\partial G_i$, trivially vanishes and the full propagators are equal to the tree-level propagators. The thermodynamic pressure is, up to a sign, identical to the value of the effective potential at its minimum,

$$p = -V_{\text{eff}}(\phi, \alpha_0, G_\sigma, G_\pi, G_\alpha), \quad (22)$$

where ϕ, α_0, G_i are the solutions of the gap equations (19), (20), (21).

The effective potential in Eq. (17) depends on the physical field ϕ and the auxiliary field α_0 . Furthermore, it has the shape of a saddle. Therefore the solutions of the gap equations (19), (20), (21) correspond to a saddle point and not to the global minimum of Eq. (17). Since the auxiliary field is not an independent dynamical degree of freedom but a Lagrange multiplier, the condensate equation for α_0 serves only as an additional constraint on the thermodynamics of the model. Substituting $i\alpha_0$ in Eqs. (15) and (19) by the right-hand side of Eq. (20) gives the following equations for the physical condensate ϕ and the masses

$$\begin{aligned} h &= \phi \left[M_\pi^2(\varepsilon, h) + \frac{4}{N\varepsilon} \int_k G_\sigma(k) \right], \\ M_\sigma^2(\varepsilon, h) &= M_\pi^2(\varepsilon, h) + \frac{4\phi^2}{N\varepsilon}, \\ M_\pi^2(\varepsilon, h) &= \frac{2}{N\varepsilon} \left[\phi^2 - v_0^2 + \int_k G_\sigma(k) + (N-1) \int_k G_\pi(k) \right]. \end{aligned} \quad (23)$$

This set of equations will be referred to as ‘‘Hartree approximation’’ in the following. Neglecting terms which are subleading in $1/N$ — an approximation commonly referred to as the large- N limit — the gap equations reduce to

$$\begin{aligned} h &= \phi M_\pi^2(\varepsilon, h) + \mathcal{O}(N^{-1}), \\ M_\sigma^2(\varepsilon, h) &= M_\pi^2(\varepsilon, h) + \frac{4\phi^2}{N\varepsilon}, \\ M_\pi^2(\varepsilon, h) &= \frac{2}{N\varepsilon} \left[\phi^2 - v_0^2 + N \int_k G_\pi(k) \right] + \mathcal{O}(N^{-1}). \end{aligned} \quad (24)$$

Note that the condensate and the v.e.v. are $\sim \sqrt{N}$, i.e., $\phi^2 \sim v_0^2 \sim N$.

Furthermore, after substituting the auxiliary field in Eq. (17) using Eq. (20), we obtain the usual ‘‘Mexican hat’’ shape for the effective potential:

$$\begin{aligned} V_{\text{eff}}(\phi, G_\sigma, G_\pi) &= \frac{1}{2N\varepsilon}(\phi^2 - v_0^2)^2 - h\phi + \frac{1}{2} \sum_{i=\sigma, \pi} \int_k [\ln G_i^{-1}(k) + D_i^{-1}(k; \phi) G_i(k) - 1] \\ &+ \frac{1}{2N\varepsilon} \left[\int_k G_\sigma(k) \right]^2 + \frac{(N-1)^2}{2N\varepsilon} \left[\int_k G_\pi(k) \right]^2 + \frac{N-1}{N\varepsilon} \int_k G_\pi(k) \int_q G_\sigma(q). \end{aligned} \quad (25)$$

Finally, we present for comparison the results for the effective potential that one obtains by a direct application of the CJT formalism to the original Lagrangian \mathcal{L}_σ of the $O(N)$ linear σ -model, Eq. (5), where no auxiliary field is present:

$$V_{\text{eff}}^{\text{CJT}}(\phi, G_\sigma, G_\pi) = \frac{1}{2N\varepsilon}(\phi^2 - v_0^2)^2 - h\phi + \frac{1}{2} \sum_{i=\sigma, \pi} \int_k [\ln G_i^{-1}(k) + D_i^{-1}(k; \phi) G_i(k) - 1] + V_2^{\text{CJT}}(G_\sigma, G_\pi), \quad (26)$$

where

$$V_2^{\text{CJT}}(G_\sigma, G_\pi) = \frac{3}{2N\varepsilon} \left[\int_k G_\sigma(k) \right]^2 + (N+1) \frac{N-1}{2N\varepsilon} \left[\int_k G_\pi(k) \right]^2 + \frac{N-1}{N\varepsilon} \int_k G_\pi(k) \int_q G_\sigma(q). \quad (27)$$

The expression for V_2^{CJT} is rather similar to the last line of Eq. (25), except for the combinatorial prefactors. However, as we shall comment in the next section, the numerical results using the effective potential (26) differ sizably from the ones obtained using the effective potential (25).

In Ref. [32], Ivanov, Riek, and Knoll introduced a heuristic modification of the CJT result (25), which is constructed such that Goldstone's theorem is preserved. In our notation,

$$\begin{aligned} V_2^{\text{IRK}}(G_\sigma, G_\pi) &= V_2^{\text{CJT}}(G_\sigma, G_\pi) - \frac{N-1}{N\varepsilon} \left\{ \int_k [G_\pi(k) - G_\sigma(k)] \right\}^2 \\ &= \frac{5-2N}{2N\varepsilon} \left[\int_k G_\sigma(k) \right]^2 + \frac{(N-1)^2}{2N\varepsilon} \left[\int_k G_\pi(k) \right]^2 + \frac{3(N-1)}{N\varepsilon} \int_k G_\pi(k) \int_q G_\sigma(q). \end{aligned} \quad (28)$$

Note that the coefficient of the term containing two pion loops is the same as in Eq. (25), although all other terms have different coefficients. However, in the large- N limit, all approaches give the same result for the effective potential.

Carrying out the Matsubara summation of the tadpole integrals gives

$$\int_k G_i(k) = \int \frac{d^3\vec{k}}{(2\pi)^3} \frac{1}{2\sqrt{\vec{k}^2 + M_i^2}} \left[1 + \frac{2}{\exp\left(\sqrt{\vec{k}^2 + M_i^2}/T\right) - 1} \right]. \quad (29)$$

Note that the vacuum contribution of Eq. (29) can be written as

$$\bar{Q}_\mu \equiv \int \frac{d^3\vec{k}}{(2\pi)^3} \frac{1}{2\sqrt{\vec{k}^2 + M^2}} = \int \frac{d^4k}{(2\pi)^4} \frac{1}{k^2 + M^2}. \quad (30)$$

This term, however, exhibits quadratic and logarithmic divergences and thus has to be regularized,

$$\bar{Q}_\mu \longrightarrow Q_\mu = \int \frac{d^4k}{(2\pi)^4} \left[\frac{1}{k^2 + M^2} - \frac{1}{k^2 + \mu^2} - \frac{\mu^2 - M^2}{(k^2 + \mu^2)^2} \right] = \frac{\mu^2}{(4\pi)^2} \left[\frac{M^2}{\mu^2} \ln\left(\frac{M^2}{\mu^2}\right) - \frac{M^2}{\mu^2} + 1 \right], \quad (31)$$

where μ is the renormalization scale. We choose to put $\mu = m_\sigma$ for the following reason. In the vacuum and in the chiral limit, $h \rightarrow 0^+$, the pion mass vanishes, $m_\pi \rightarrow 0^+$. Then, the first equation (23) requires that the vacuum contribution to the tadpole integral $\int_k G_\sigma(k)$ vanishes. From the result (31) we observe that this can only be realized with the choice $\mu = m_\sigma$. Note that Q_μ is always positive semi-definite, irrespective of the value of M^2/μ^2 .

IV. RESULTS

In this section, we show numerical solutions of Eqs. (23) and (24) for $N = 4$, corresponding to a system of three pions and their chiral partner, the σ particle. We discuss the results for the linear and the nonlinear σ -model, with and without explicitly broken chiral symmetry. Furthermore, we investigate different renormalization schemes, i.e., the above mentioned counter-term renormalisation (CTR) method, Eq. (31), and a so-called trivial renormalisation (TR) where the vacuum contribution Q_μ of the tadpole integral is set to zero.

A. Linear model with explicitly broken symmetry

In Fig. 1 we show the masses of the pion and the sigma, as well as the condensate as a function of temperature for different values of the vacuum sigma mass m_σ . One observes that the condensate decreases as a function of temperature, which is a consequence of the restoration of chiral symmetry. Depending on the value of m_σ , chiral symmetry restoration may proceed via a phase transition. In the CTR scheme, the phase transition is of second order for $m_\sigma \simeq 500$ MeV, and of first order for larger values of m_σ . For smaller values, however, the transition is only crossover. In the chirally restored phase, the condensate is always nonzero because of the small explicit breaking of chiral symmetry due to non-vanishing quark masses (or, equivalently, $m_\pi = 139.5$ MeV). Since the results for the TR scheme are qualitatively similar, we do not show them explicitly, but we remark that the second-order transition occurs for larger values of the vacuum sigma mass, $m_\sigma \simeq 700$ MeV. Note that a crossover transition is also found in lattice QCD calculations [3]. However, it should be stressed that in QCD the identification of the chiral partner of the pion is a long-debated issue, see Refs. [33] and refs. therein.

Figure 2 shows the effect of different renormalization and approximation schemes on the behavior of the masses and the condensate as functions of temperature. We keep the vacuum mass of the sigma fixed to $m_\sigma = 550$ MeV. In the

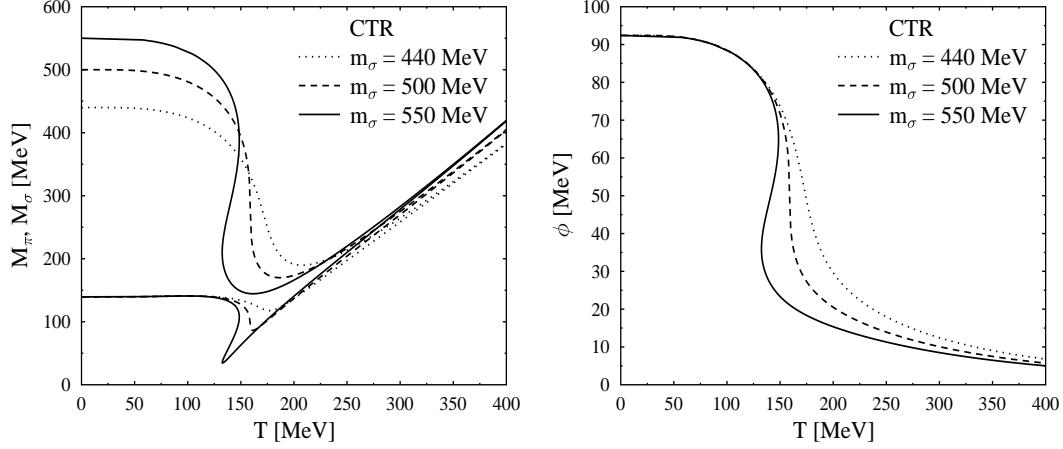


FIG. 1: The pion mass, the sigma mass, and the condensate as a function of T in the $O(4)$ linear model in case of explicitly broken symmetry using the CTR scheme for different values of m_σ .

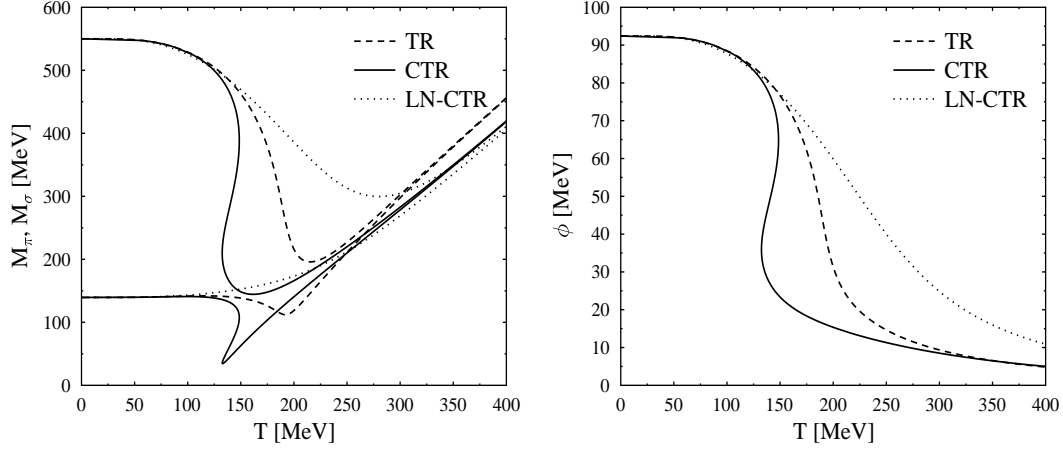


FIG. 2: The pion mass, the sigma mass, and the condensate as a function of T in the $O(4)$ linear model in case of explicitly broken symmetry for $m_\sigma = 550$ MeV and different renormalization schemes.

CTR scheme, the system exhibits a first-order phase transition. When using the TR scheme, however, one observes a crossover transition. In the large- N limit with CTR, the chiral transition is always crossover, independent of the mass of the σ . In Fig. 2, the crossover transition is observed to be smoother for the large- N approximation with CTR than for the other cases. In fact, with this renormalization scheme, the smoothness is proportional to m_σ . We shall see in the next section that the transition disappears as we approach the nonlinear limit $m_\sigma \rightarrow \infty$. This, however, does not happen for the TR scheme.

B. Nonlinear model with explicitly broken symmetry

The results for the nonlinear model are obtained by taking the limit $\varepsilon \rightarrow 0^+$. Because of the relation (15), $1/\varepsilon = (m_\sigma^2 - m_\pi^2)/\phi^2$, the nonlinear limit is equivalent to sending m_σ to infinity.

In this case, in the Hartree approximation and when the TR scheme is used, the phase transition is of first order, with a rather large discontinuity in the condensate at the critical temperature of $T_c \simeq 178.6$ MeV, see Fig. 3. The condensate is very small above T_c , but still nonzero, because of explicit symmetry breaking. The first-order nature of the transition is in line with the expectation from the linear case, where the transition becomes first order when the

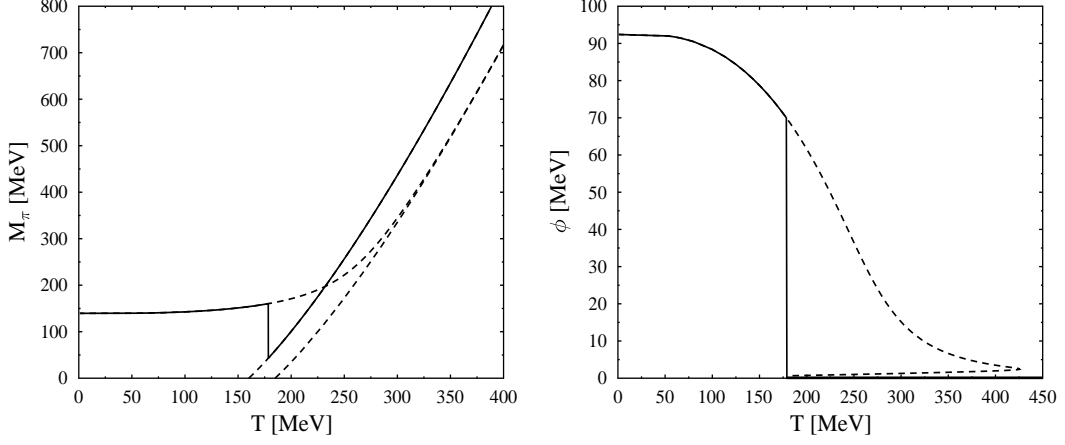


FIG. 3: The pion mass and the condensate as a function of T in the $O(4)$ nonlinear model in case of explicitly broken symmetry using the Hartree-approximation in the TR-scheme for $m_\sigma \rightarrow \infty$ (in practice $m_\sigma = 250$ MeV is used). The solid line corresponds to the physical case. The dashed line corresponds to the unstable or metastable solution of the gap equations.

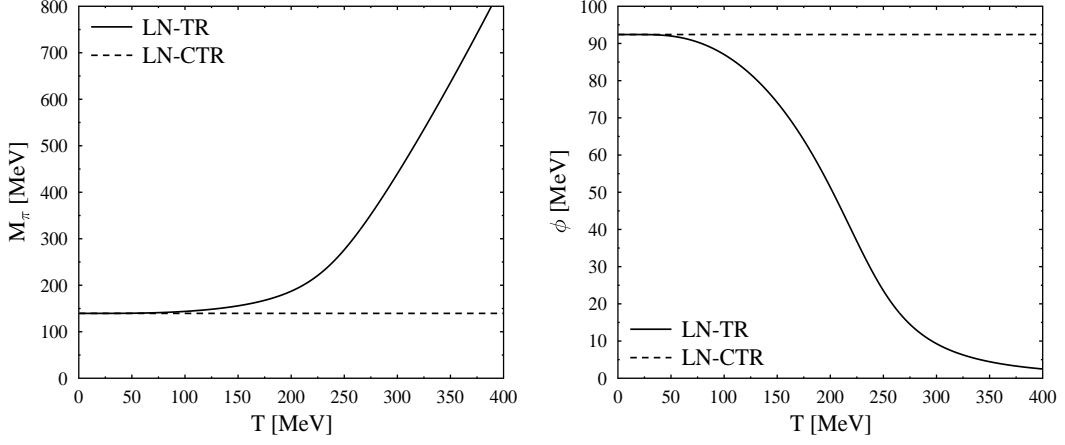


FIG. 4: The pion mass and the condensate as a function of T in the $O(4)$ nonlinear model in case of explicitly broken symmetry using the LN-approximation in the TR-scheme (full) and CTR-scheme (dashed) for $m_\sigma \rightarrow \infty$.

σ mass is sufficiently large. Below T_c the σ mass is infinitely heavy and there are only pionic excitations. Above T_c the masses of σ and π become degenerate.

In the large- N approximation and with the TR scheme, the phase transition is crossover with $T_c \simeq 185$ MeV, see Fig. 4. In this case the σ field remains infinitely heavy also above T_c . This is the main difference to the Hartree case, where the σ becomes degenerate with the π above T_c . It is at first sight surprising that this small difference can cause such a drastic change in the order of the phase transition. The explanation lies in a comparison of the gap equations (23) in the Hartree approximation with those in the large- N limit, Eqs. (24). Since the σ is infinitely heavy below T_c , there is no contribution from this mode to the gap equations. However, above T_c , thermal fluctuations of the σ can contribute in the Hartree approximation, while they remain absent in the large- N limit. This is sufficient to drive the transition to first order in the Hartree approximation.

In the CTR scheme, the parameter space of the model does not allow for physical solutions in the nonlinear case $m_\sigma \rightarrow \infty$. In the Hartree approximation, $\phi \rightarrow 0$ and $M_\sigma, M_\pi \rightarrow \infty$ for all values of T . In the large- N approximation, the transition disappears completely, the condensate and the masses retain their constant tree-level values for all $T > 0$: $\phi = f_\pi$, $M_\sigma = m_\sigma$, $M_\pi = m_\pi$, see Fig. 4.

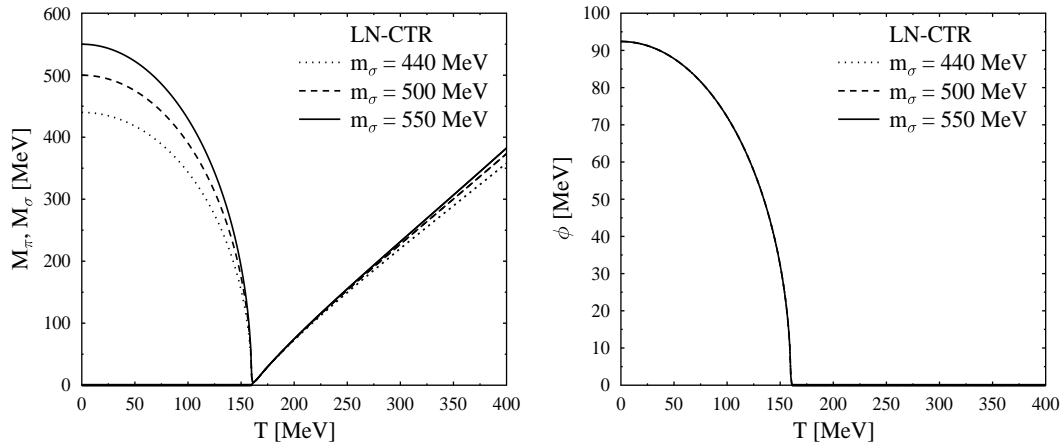


FIG. 5: The pion mass, the sigma mass and the condensate as a function of T in the $O(4)$ linear model in the chiral limit.

C. Linear model in the chiral limit

The chiral limit is obtained by taking $m_\pi \rightarrow 0^+$. In this case, the first equation (23) requires that the σ -tadpole exactly cancels M_π^2 . This, however, is only possible, if the pion becomes tachyonic, $M_\pi^2 < 0$, since the thermal as well as the vacuum contribution (31) to the tadpole are always positive (semi-)definite. As a consequence, we can only show results in the large- N limit, since there this problem is absent, cf. Eqs. (24).

In Fig. 5 we show the behavior of the masses and the condensate as functions of temperature for various values of the vacuum sigma mass in the large- N limit in the CTR scheme (the results for TR scheme are qualitatively similar, therefore we do not show them explicitly). The results of Fig. 5 are in agreement with universality class arguments which predict a second-order phase transition. In the phase where chiral symmetry is spontaneously broken the pions are massless in accordance with Goldstone's theorem. Above the critical temperature the chiral partners become degenerate in mass. The condensate as a function of temperature is independent of the value of m_σ . This can be seen as follows. We subtract the last equation (24) at $T = 0$ (where $\phi = f_\pi$) from the same equation at an arbitrary temperature $T \leq T_c$, where T_c is the phase transition temperature. Since in the phase of broken chiral symmetry we always have $M_\pi \equiv 0$, the result is

$$0 = \phi^2(T) - f_\pi^2 + N \frac{T^2}{12}, \quad (32)$$

where the thermal contribution to the tadpole integral could be determined analytically at all temperatures because $M_\pi = 0$. The term v_0^2 , as well as the vacuum contributions to the tadpole integrals (which depend on m_σ) cancel when taking the difference. The critical temperature T_c can be easily deduced from Eq. (32) noting that $\phi(T_c) = 0$. The result is $T_c = \sqrt{12/N} f_\pi = \sqrt{3} f_\pi$.

D. Nonlinear model in the chiral limit

In the chiral limit of the nonlinear $O(N)$ model both parameters ε and h must be sent to zero. In the Hartree approximation and in the TR scheme, pions respect Goldstone's theorem by remaining massless in the phase of spontaneously broken chiral symmetry, see Fig. 6. In this phase, the σ -field is effectively frozen out due to its infinite mass. There is a first-order phase transition at a critical temperature $T_c = \sqrt{3} f_\pi$. At this temperature, the condensate drops to zero discontinuously, while the pion mass starts to increase continuously from zero above this temperature. In the restored phase, the σ becomes degenerate in mass with the pions. This is the reason why T_c assumes the same value as in the large- N limit of the linear model. When inspecting the gap equations (23), we observe that they become identical with Eqs. (24) for $M_\sigma = M_\pi = 0$ in the chiral limit and above T_c (where $\phi = 0$). Therefore, we obtain the same equation (32) that determines the value of T_c as in the linear case in the large- N limit.

However, when applying the Hartree approximation in the CTR scheme no physical solutions can be obtained: the condensate goes to zero, $\phi \rightarrow 0$, and the masses of sigma and pion go to infinity, $M_\sigma, M_\pi \rightarrow \infty$. This situation is similar to the nonlinear case with explicit symmetry breaking.

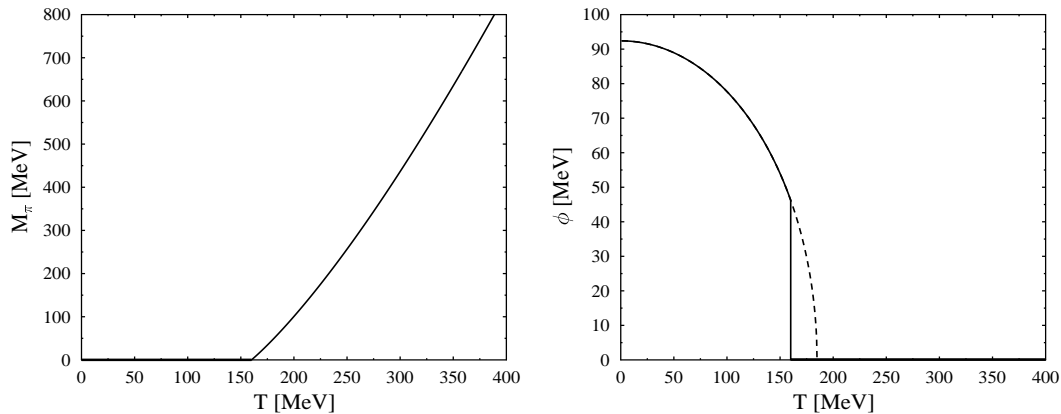


FIG. 6: The pion mass and the condensate as a function of T in the $O(4)$ nonlinear model in the chiral limit in the TR-scheme and Hartree-approximation for $m_\sigma \rightarrow \infty$ (in practice $m_\sigma = 250$ MeV is used). The solid line corresponds to the physical case. The dashed line corresponds to the unstable or metastable solution of the gap equations.

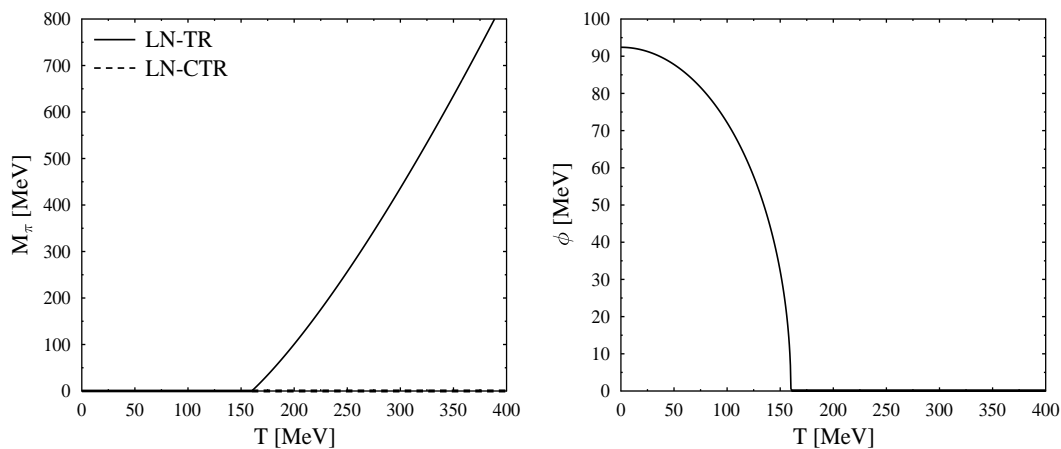


FIG. 7: The pion mass and the condensate as a function of T in the $O(4)$ nonlinear model in the chiral limit using the LN-approximation in the TR-scheme (full) and CTR-scheme (dashed) for $m_\sigma \rightarrow \infty$.

In the large- N approximation, the phase transition is of second order with a critical temperature $T_c = \sqrt{3}f_\pi$, both in the TR and in the CTR scheme, see Fig. 7. Below T_c the σ mass is infinite, while the pions are massless, respecting Goldstone's theorem. Above the critical temperature the masses of the chiral partners become degenerate, $M_\sigma = M_\pi > 0$ in the TR scheme, and $M_\sigma = M_\pi = 0$ in the CTR scheme. At first sight, it is surprising that the σ field becomes massless above T_c . This behavior can be traced to our choice of the renormalization scale $\mu = m_\sigma \rightarrow \infty$. In fact, this is similar to what was observed in Ref. [13] (cf. Fig. 3 of that work), when increasing the renormalization scale in the large- N limit in the CTR scheme.

V. CONCLUSIONS

In this work we have investigated the linear and the nonlinear $O(N)$ model at nonzero temperature. An auxiliary field has been used to derive the effective potential. This method allowed us to establish a simple and mathematically rigorous relation between the linear and nonlinear versions of the model. This also leads to differences when comparing our results with previous treatments of the $O(N)$ model, see below. The gap equations for the temperature-dependent masses and the condensate were derived using the CJT formalism. To regularize the divergent vacuum terms we applied

	CTR	CTR	TR	TR	LN-CTR	LN-CTR	LN-TR	LN-TR
	$m_\pi = m_\pi^{phys}$	$m_\pi \rightarrow 0^+$	$m_\pi = m_\pi^{phys}$	$m_\pi \rightarrow 0^+$	$m_\pi = m_\pi^{phys}$	$m_\pi \rightarrow 0^+$	$m_\pi = m_\pi^{phys}$	$m_\pi \rightarrow 0^+$
lin	second order at $m_\sigma \simeq 500$ MeV	\otimes	second order at $m_\sigma \simeq 750$ MeV	\otimes	crossover	second order $T_c = \sqrt{\frac{12}{N}} f_\pi$	crossover	second order $T_c = \sqrt{\frac{12}{N}} f_\pi$
nonlinear	\otimes	\otimes	first order	first order $T_c = \sqrt{\frac{12}{N}} f_\pi$	no transition	second order $T_c = \sqrt{\frac{12}{N}} f_\pi$	crossover	second order $T_c = \sqrt{\frac{12}{N}} f_\pi$

TABLE I: The symbol \otimes indicates that no reasonable result can be obtained due to tachyonic pion propagation. In those cases the phase transition becomes cross-over for smaller sigma masses and of first order for sigma masses higher than the shown values. $m_\pi = m_\pi^{phys}$ corresponds to the physical case of nonzero quark masses, $m_\pi^{phys} = 139.5$ MeV.

the counter-term method (CTR scheme) as well as the so-called trivial regularization (TR scheme) where divergent terms are simply ignored.

Table I shows a compilation of the results for the various scenarios studied in this paper. The first row summarizes the results for the linear case, while the second those for the nonlinear case. In the first four columns we show the results for the Hartree approximation, the first two for the CTR and the next two for the TR scheme, for the case of explicit chiral symmetry breaking and in the chiral limit. The last four columns show the corresponding results for the large- N limit. In the cases indicated with a \otimes , we were not able to find physically acceptable solutions due to tachyonic pion propagation. In all other cases, we indicated the nature of the phase transition and, if independent of the σ mass, the critical temperature. As one observes, $T_c = \sqrt{12/N} f_\pi \equiv \sqrt{3} f_\pi$ in the chiral limit for all scenarios, independent of the details (linear vs. nonlinear, or CTR vs. TR, or Hartree vs. large- N). In the cases where the order of the transition depends on the σ mass, we indicated the value of m_σ where the transition is of second order; it is crossover for smaller and of first order for larger values of m_σ .

We now compare our results to previous work. In Ref. [13], the $O(N)$ model for $N = 4$ was studied in the CJT formalism without using the auxiliary field method. Although not studied in that work, we repeated the respective calculations varying the σ mass. We find that, in the Hartree approximation and in the case of explicitly broken chiral symmetry, the phase transition changes from crossover to first order for $m_\sigma \simeq 940$ MeV in the TR scheme and for $m_\sigma \simeq 680$ MeV in the CTR scheme. This is consistent with our results obtained with the auxiliary field method, although the critical values for m_σ are somewhat larger for the method of Ref. [13]. In the chiral limit, the method of Ref. [13] yields a first-order phase transition for all m_σ values. Furthermore, Goldstone's theorem is not fulfilled due to a non-vanishing pion mass in the phase of broken chiral symmetry. In the large- N limit, the results of Ref. [13] coincide with ours, since the effective potentials are identical, cf. remark after Eq. (28).

The auxiliary field method has been applied previously to examine properties of the $O(N)$ model to leading [27, 28] and next-to-leading order in the $1/N$ expansion [29, 30]. To leading order in $1/N$ the σ and π fields have the same mass irrespective of whether chiral symmetry is explicitly or only spontaneously broken. Thus, in the chiral limit there are four instead of three massless bosons. The phase transition is of second order with a critical temperature of $T_c = \sqrt{12/N} f_\pi$. In the case of explicitly broken symmetry there is a crossover phase transition and four massive particles. To next-to-leading order including renormalization [29] the results change as follows: in the chiral limit there are three Goldstone bosons since the σ -field becomes massive. The phase transition is of second (or higher) order. In the weak-coupling limit the critical temperature is $T_c = \sqrt{12/(N+2)} f_\pi$ and above the critical temperature the masses of the chiral partners become degenerate. The key difference in our study to the afore mentioned Refs. [27, 28] is the correct treatment of the limiting process regarding the constraint imposed by the nonlinearity: the σ -mass is therefore infinite in the phase of broken symmetry.

A natural next step is to include sunset-type diagrams in the CJT effective action, which lead to nonzero imaginary parts for the self-energy of the quasiparticles and, in turn, to a nonzero decay width [16]. Another project is the extension to nonzero chemical potentials [30]. A further interesting study would be the inclusion of additional scalar singlet states, since the nature of their constituency is quite unclear [34]. Finally, the application of the auxiliary field method should also be instructive for more complicated systems incorporating additional vector and axial vector mesonic degrees of freedom [35].

Acknowledgement

The authors thank T. Brauner, M. Grahl, A. Heinz, S. Leupold, and H. Warringa for interesting discussions. The

work of E. Seel was supported by the Helmholtz Research School “H-QM”.

-
- [1] G. 't Hooft, Phys. Rept. **142**, 357 (1986).
 - [2] C. Vafa and E. Witten, Nucl. Phys. B **234**, 173 (1984).
 - [3] Proc. of LATTICE '96, Nucl. Phys. B **53** (Proc. Suppl.), 1 (1997).
 - [4] R. D. Pisarski and F. Wilczek, Phys. Rev. D **29**, 338 (1984).
 - [5] L. Dolan and R. Jackiw, Phys. Rev. D **9**, 2904 (1974).
 - [6] E. Braaten and R. D. Pisarski, Nucl. Phys. B **337**, 569 (1990).
 - [7] J. M. Cornwall, R. Jackiw and E. Tomboulis, Phys. Rev. D **10**, 2428 (1974).
 - [8] G. Baym and L. P. Kadanoff, Phys. Rev. **124**, 287 (1961).
 - [9] J. M. Luttinger and J. C. Ward, Phys. Rev. **118**, 1417 (1960).
 - [10] G. Baym, Phys. Rev. **127**, 1391 (1962).
 - [11] H. van Hees and J. Knoll, Phys. Rev. D **66**, 025028 (2002).
 - [12] N. Petropoulos, J. Phys. G **25**, 2225 (1999).
 - [13] J. T. Lenaghan and D. H. Rischke, J. Phys. G **26**, 431 (2000).
 - [14] S. Chiku and T. Hatsuda, Phys. Rev. D **58**, 076001 (1998); S. Chiku Prog. Theor. Phys. **104**, 1129 (2000).
 - [15] J. T. Lenaghan and D. H. Rischke, J. Phys. G **26**, 431 (2000).
 - [16] D. Roder, J. Ruppert and D. H. Rischke, Phys. Rev. D **68**, 016003 (2003).
 - [17] G. Baym and G. Grinstein, Phys. Rev. D **15**, 2897 (1977).
 - [18] J. Polchinski, arXiv:hep-th/9611050.
 - [19] G. Amelino-Camelia and S. Y. Pi, Phys. Rev. D **47**, 2356 (1993).
 - [20] G. Amelino-Camelia, Phys. Lett. B **407**, 268 (1997).
 - [21] H. S. Roh and T. Matsui, Eur. Phys. J. A **1**, 205 (1998).
 - [22] Y. Nemoto, K. Naito and M. Oka, Eur. Phys. J. A **9**, 245 (2000).
 - [23] N. Petropoulos, arXiv:hep-ph/0402136.
 - [24] D. Roder, J. Ruppert and D. H. Rischke, Nucl. Phys. A **775**, 127 (2006).
 - [25] S. R. Coleman, R. Jackiw and H. D. Politzer, Phys. Rev. D **10**, 2491 (1974).
 - [26] R. G. Root, Phys. Rev. D **10**, 3322 (1974).
 - [27] H. Meyers-Ortmanns, H. J. Pirner and B. J. Schaefer, Phys. Lett. B **311**, 213 (1993).
 - [28] A. Bochkarev and J. I. Kapusta, Phys. Rev. D **54**, 4066 (1996).
 - [29] J. O. Andersen, D. Boer and H. J. Warringa, Phys. Rev. D **70**, 116007 (2004).
 - [30] J. O. Andersen and T. Brauner, Phys. Rev. D **78**, 014030 (2008).
 - [31] R.J. Rivers, Path integral methods in quantum field theory (Cambridge University Press, Cambridge, 1987).
 - [32] Yu. B. Ivanov, F. Riek and J. Knoll, Phys. Rev. D **71**, 105016 (2005); Yu. B. Ivanov, F. Riek, H. van Hees and J. Knoll, Phys. Rev. D **72**, 036008 (2005).
 - [33] C. Amsler and N. A. Tornqvist, Phys. Rept. **389**, 61 (2004); E. Klempt and A. Zaitsev, Phys. Rept. **454**, 1 (2007); F. Giacosa, Phys. Rev. D **80**, 074028 (2009).
 - [34] A. Heinz, S. Struber, F. Giacosa and D. H. Rischke, Acta Phys. Polon. Supp. **3**, 925 (2010).
 - [35] S. Strueber and D. H. Rischke, Phys. Rev. D **77** (2008) 085004; D. Parganlija, F. Giacosa and D. H. Rischke, Phys. Rev. D **82** (2010) 054024; D. Parganlija, F. Giacosa and D. H. Rischke, Phys. Rev. D **82**, 054024 (2010); S. Gallas, F. Giacosa and D. H. Rischke, Phys. Rev. D **82**, 014004 (2010).